On the dimensioning of cellular OFDMA networks

Jean-Marc Kélif, Marceau Coupechoux, Philippe Godlewski

On the Dimensioning of Cellular OFDMA Networks

Jean-Marc Kelif[a], Marceau Coupechoux[*,b], Philippe Godlewski[b]

[a] *Orange Labs, 38 av. du Gal Leclerc, 92794 Issy-les-Moulineaux, France*
[b] *Telecom ParisTech and CNRS LTCI, 23 av. d'Italie, 75013 Paris, France*

Abstract

In this paper, we address the issue of cellular OFDMA networks dimensioning. Network design consists of evaluating cell coverage and capacity and may involve many parameters related to environment, system configuration, and quality of service (QoS) requirements. In order to quickly study the impact of each of these parameters, analytical formulas are needed. The key function for network dimensioning is the Signal to Interference Ratio (SIR) distribution. We thus analyze in an original way the traditional issue of deriving outage probabilities in OFDMA cellular networks. Our study takes into account the joint effect of path-loss, shadowing, and fast fading effects. Starting from the Mean Instantaneous Capacity (MIC), we derive the effective SIR distribution as a function of the number of sub-carriers per sub-channel. Our formula, based on a fluid model approach, is easily computable and can be obtained for a mobile station (MS) located at any distance from its serving base station (BS). We validate our approach by comparing all results to Monte Carlo simulations performed in a hexagonal network, and

[*]corresponding author, +33 1 45 81 75 88
Email addresses: jeanmarc.kelif@orange-ftgroup.com (Jean-Marc Kelif), coupecho@enst.fr (Marceau Coupechoux), godlewsk@enst.fr (Philippe Godlewski)

we show how our analytical study can be used to analyze outage capacity, coverage holes, and network densification. The proposed framework is a powerful tool to study performances of cellular OFDMA networks (e.g. WiMAX, LTE).

Key words: Cellular networks, OFDMA, SINR, Dimensioning, Cell breathing, Network densification

1. Introduction

All cellular systems of the fourth generation will adopt Orthogonal Frequency Division Multiple Access (OFDMA) as the basis for their multiple-access scheme on the downlink. In OFDMA, the system bandwidth is subdivided into sub-carriers, which are grouped to form sub-channels. A sub-channel is, in turn, the elementary frequency radio resource that can be allocated to a user.

As WiMAX networks are being deployed and first experiments of Long Term Evolution (LTE) are underway, the need arises for cellular operators to get efficient dimensioning tools for OFDMA networks. The key function for network design is the Signal to Interference plus Noise Ratio (SINR) distribution. On the one hand, radio coverage is indeed defined as the probability that SINR at cell edge is above a given threshold. On the other hand, capacity and traffic studies in cellular networks very often rely on the Modulation and Coding Scheme (MCS) probabilities, which can be directly derived from the SINR Cumulative Distribution Function (CDF), or, alternatively on the Shannon formula, which depends also on the SINR (see e.g. [16]).

In this paper, we address in an original way the traditional issue of de-

riving outage probabilities in cellular networks. We focus on an urban environment so that the SINR can be approximated by the Signal to Interference Ratio (SIR). First, we propose a simple approximation of the SIR CDF on a generic sub-carrier at any distance of the Base Station (BS), while taking into account the joint effect of path-loss, shadowing and fast fading. Outage probabilities can thus be obtained at a click speed with very good accuracy. Then, we extend this approach to OFDMA networks, for which the notions of Mean Instantaneous Capacity (MIC) and effective SIR have been introduced. Effective SIR CDF is obtained as a function of the number of sub-carriers per sub-channel.

The issue of expressing outage probability in cellular networks has been extensively addressed in the literature. For such a study, there are often two possible assumptions: (1) considering only the shadowing effect, (2) considering both shadowing and fast fading effects. In the former case, authors mainly face the problem of expressing the distribution of the sum of log-normally random variables; several classical methods can be applied to solve this issue (see e.g. [12] [3]). In the latter case, formulas usually consist of many infinite integrals, which are uneasy to handle in practice (see e.g. [13]). In both cases, outage probability is expressed as an explicit function of the distances between the user and all interferers. Such multivariate functions are difficult to handle and to integrate in practice for dimensioning purposes.

As the need for easy-to-use formulas for outage probability is clear, approximations need to be done. Working on the uplink, [11] derived the distribution function of a ratio of received powers at the base-station by considering path-loss and shadowing; it is an essential result for the evaluation of

external interference. For that, authors approximate the hexagonal cell with a disk of same area. On the downlink, Chan and Hanly [9] precisely approximate the distribution of the other-cell interference. They however provide formulas that are difficult to handle in practice and do not consider fast fading. Immovilli and Merani [15] take into account the two channel effects and make several assumptions in order to obtain simplified formulas. In particular, they approximate interference by its mean value. Outage probability is however again expressed as an explicit function of the distances from receiver to every interferer. Zorzi, in [17], proposes a simple formula but for packet radio networks rather than for cellular systems. Reference [18] provides some interesting characterizations and upper bounds of the outage probability but neglects the slowly varying path-gains. In [19], authors consider both shadowing and fast fading but assume a single interferer.

In the context of OFDMA access, many papers deal with the resource allocation problem on the downlink, which consists of allocating power and sub-carriers to multiple users in order to maximize the cell sum rate (see e.g. [27, 28]). Performance analysis assuming limited or erroneous feedback channel has also received a lot of interest in recent years, see e.g. [25] and references therein. Most of these papers, which often rely on the computation of outage probabilities, however neglect inter-cell interference and focus on Signal to Noise (SNR) variations. Two notable exceptions are references [26] and [29]. The former considers only a two cell network. The latter derives an expression of the SINR distribution conditionally on the average received powers and rely on Monte Carlo simulations at cell edge to obtain the symbol error rate.

Concerning the dimensioning of OFDMA networks, many papers (e.g. [30]) are studying system performance based on simulations, which are more or less following the instructions provided in methodology documents such as [22]. Few papers are dealing with analytical approaches. Although [20] studies outage probability as a function of the system load, whereas we are considering only a fully loaded system, the proposed analytical expression explicitly depends on all distances to interferers. A paper close in its objectives to our work is [21]. A simple planning procedure is proposed based on the evaluation of two averages of the SINR. Effective SINR is approximated by a Gaussian random variable (RV). The limitation of this study lies in the fact that the two involved averages are computed by simulations and have to be obtained for each user location.

In order to calculate the SIR distribution, while taking into account shadowing, we approximate a sum of log-normal RV by a log-normal RV using the Fenton-Wilkinson method. Then, we jointly take into account shadowing and fast fading and derive an outage probability formula, for a mobile located at any distance from its serving BS. At last, we rely on a recently proposed fluid model [5] in order to express the outage probability as a function of the distance to the serving BS. Such an expression allows further integrations much more easily than with existing formulas. We then extend this result to OFDMA networks by approximating the effective SIR by a log-normal RV, whose parameters can be easily computed. Our approach is validated by Monte Carlo simulations.

The fluid model has been originally proposed in [5]. It has been shown in [6] how this model can be efficiently used for admission control. In [7] and

[8], we have used the fluid model in order to compute outage probability and spatial outage probability in CDMA cellular networks for a simple propagation model only based on path-loss. In this paper, we extend this work by adapting the model to OFDMA networks and by considering shadowing and fast fading.

In the next section, we introduce the interference and network model and give the SIR definition. In Section 3, we derive outage probability for multi-carrier systems. We first present the MIC approach, then derive the SIR CDF on a generic sub-carrier and at last derive the effective SIR distribution. We also apply in this section the fluid model in order to obtain an interference factor needed to compute SIR CDFs. Our analytical approach is validated by Monte Carlo simulations in Section 4. An example of dimensioning involving a streaming service is given in Section 5: studies of the outage capacity, coverage holes and network densification are performed with our formulas. At last, Section 6 concludes the paper.

2. Signal to Interference Ratio and Outage Definitions

We consider a homogeneous cellular network and focus on a mobile station (MS) u and its serving base station (BS), BS_0, surrounded by N interfering BS. We describe in this section the interference models used in this paper.

On the downlink, the power received by MS u can be described by the three stage propagation model that considers path-loss, shadowing effect, and fast fading. Let P_j be the transmission power of BS j, the power $p_{j,u}$ received by u can thus be written as:

$$p_{j,u} = P_j K r_{j,u}^{-\eta} X_{j,u} Y_{j,u}. \tag{1}$$

The path-loss model is characterized by parameters K and $\eta > 2$ (typically between 3 and 4 in dense urban environments). The term $P_j K r_{j,u}^{-\eta}$ is the mean value of the received power at distance $r_{j,u}$ from the transmitter BS_j.

Shadowing effect is represented by random variable $Y_{j,u} = 10^{\frac{\xi_{j,u}}{10}}$, where $\xi_{j,u}$ is a normal RV, with zero mean and standard deviation σ, typically ranging from 3 to 10 dB.

RV $X_{j,u}$ is representing the Rayleigh fast fading effects, its PDF is given by $p_X(x) = e^{-x}$. In the rest of this paper, we assume that RV $\{X_{j,u}\}_{j=0,\ldots,N}$ and $\{\xi_{j,u}\}_{j=0,\ldots,N}$ are i.i.d.

For the sake of simplicity, we now drop index u and set $r_{0,u} = r$. Considering the useful power P_0 transmitted by the BS_0, the useful power p_0 received by MS u belonging to BS_0 can be written as:

$$p_0 = P_0 K r^{-\eta} Y_0 X_0. \tag{2}$$

Interference received by u coming from all the other BS of the network is expressed as:

$$p_{ext} = \sum_{j=1}^{N} P_j K r_j^{-\eta} Y_j X_j. \tag{3}$$

The SINR at user u is thus given by:

$$\gamma = \frac{P_0 K r^{-\eta} Y_0 X_0}{\sum_{j=1}^{N} P_j K r_j^{-\eta} Y_j X_j + N_{th}}, \tag{4}$$

where N_{th} is the thermal noise power. In dense urban environments, thermal noise can be neglected with respect to the co-channel interference. If we further assume that BS have identical transmitting powers, P_0, the SIR, γ

can now be written as:

$$\gamma = \frac{r^{-\eta} X_0 Y_0}{\sum_{j=1}^{N} r_j^{-\eta} X_j Y_j}. \tag{5}$$

The outage probability is now defined as the probability for the SIR γ to be lower than a threshold value δ:

$$\mathbb{P}\big(\gamma < \delta\big) = 1 - \mathbb{P}\big(p_0 > \delta p_{ext}\big). \tag{6}$$

Note that, assuming negligible noise and equal BS transmit powers, P_0 and K vanish in the outage probability expression.

3. Multi-Carrier Outage Probability

In this section, we derive an approximate formula for the outage probability of multi-carrier systems. The computation is based on the notion of Mean Instantaneous Capacity (MIC) introduced in the next section. As we then rely on the Gaussian approximation, the SIR distribution on a single carrier is needed. At last, we use the fluid model in order to obtain a simple expression of the outage probability.

3.1. Mean Instantaneous Capacity

With OFDMA, system bandwidth is made of hundreds of orthogonal narrow band sub-carriers. For example, in a 20 MHz IEEE 802.16 system, there are 2048 sub-carriers of about 11 kHz; out of them, $N_{sc}^T = 1536$ can be used for data transfer in FUSC (Full Usage of Sub Carriers) mode [23]. Because of complexity and excessive protocol overhead that it would imply, sub-carriers cannot be individually allocated to users. They are rather grouped into sub-channels and sub-channels are allocated to users. Let N_{sc} be the number of sub-carriers per sub-channel (e.g. $N_{sc} = 48$ in FUSC mode in the downlink).

As allocation is done on a sub-channel basis, quality of the signal is also evaluated per sub-channel rather than per sub-carrier. This evaluation helps the transmitter to choose the right modulation and coding scheme for link adaptation and allows the receiver to feedback an aggregated quality indicator to the transmitter. One such aggregated method is called Mean Instantaneous Capacity and is defined as [22]:

$$MIC = \frac{1}{N_{sc}} \sum_{n=1}^{N_{sc}} C_n, \tag{7}$$

where $C_n = \log_2(1 + \gamma_n)$ is the spectral efficiency in bps/Hz on sub-carrier n and γ_n is the SIR on sub-carrier n. From MIC, it is possible to define the effective SIR:

$$SIR_{eff} = 2^{MIC} - 1. \tag{8}$$

The effective SIR is an aggregated measure of the channel quality on a given sub-channel.

In a multi-carrier system, we define the outage probability as the probability that the effective SIR falls below a given threshold δ, $\mathbb{P}\big(SIR_{eff} < \delta\big)$. As N_{sc} is typically greater than 10, it is clear that the RV MIC can be approximated by a normally distributed RV. As a consequence, the distribution of C_n and thus of γ_n (the SIR on a generic single carrier) are needed in order to compute the first and second moment of the MIC.

Remark 1: Expression of C_n reflects the spectral efficiency formula for an AWGN (Average White Gaussian Noise) channel. Shannon capacity of channels with interference is an open problem in information theory (see chapter 15 of [31]). The approximation $\log(1 + \gamma)$ is however often used in system performance evaluation literature (assuming a worst-case for the

interference distribution, i.e., Gaussian).

3.2. Single Carrier Study

In this section, we focus on a single generic sub-carrier. Using Eq. 2, 3, and 6, the SIR CDF is expressed as:

$$\mathbb{P}\big(\gamma < \delta\big) = 1 - \mathbb{P}\big[r^{-\eta} X_0 Y_0 > \delta \sum_{j=1}^{N} r_j^{-\eta} X_j Y_j\big]. \tag{9}$$

We now make the simple approximation consisting of replacing RV $\{X_j\}_{j\neq 0}$ by their average values $E[X_j] = 1$ for the interfering signals. We also introduced an intermediate RV Y_f:

$$Y_f = \frac{\sum_{j=1}^{N} r_j^{-\eta} Y_j}{r^{-\eta} Y_0}. \tag{10}$$

The CDF can now be expressed as:

$$\begin{aligned}
\mathbb{P}\big(\gamma < \delta\big) &= 1 - \mathbb{P}\big(X_0 Y_0 > \frac{\delta}{r^{-\eta}} \sum_{j=1}^{N} r_j^{-\eta} Y_j\big), \\
&= 1 - \mathbb{P}\big(X_0 > \delta Y_f\big), \\
&= 1 - \int_0^{\infty} \mathbb{P}\big(x > \delta Y_f\big) p_X(x) dx, \\
&= \int_0^{\infty} \Big[1 - \mathbb{P}\left(\frac{x}{\delta} > Y_f\right)\Big] p_X(x) dx.
\end{aligned} \tag{11}$$

The factor Y_f is defined for any mobile u and is location dependent. The numerator of this factor is a sum of log-normally distributed RV, which can be approximated by a log-normally distributed RV [3]. The denominator of the factor is a log-normally distributed RV. Y_f can thus be approximated by a log-normal RV.

Using the Fenton-Wilkinson approximation [1], we can calculate the mean and standard deviation, m_f and s_f, of factor Y_f, for any mobile at distance r from its serving BS (see A).

$$m_f = \frac{1}{a}\ln(y_f(r,\eta)H(r,\sigma)), \tag{12}$$

$$s_f^2 = 2(\sigma^2 - \frac{1}{a^2}\ln H(r,\sigma)), \tag{13}$$

where $a = \frac{\ln 10}{10}$ and

$$H(r,\sigma) = e^{a^2\sigma^2/2}\left(G(r,\eta)(e^{a^2\sigma^2}-1)+1\right)^{-\frac{1}{2}}, \tag{14}$$

$$G(r,\eta) = \frac{\sum_{j\neq 0} r_j^{-2\eta}}{\left(\sum_{j\neq 0} r_j^{-\eta}\right)^2}, \tag{15}$$

$$y_f(r,\eta) = \frac{\sum_{j\neq 0} r_j^{-\eta}}{r^{-\eta}}. \tag{16}$$

We also notice that the G factor can be rewritten as a function of y_f:

$$G(r,\eta) = \frac{y_f(r,2\eta)}{y_f(r,\eta)^2}. \tag{17}$$

As a consequence, the single-carrier SIR CDF for a mobile **located at a distance r** from its serving BS, taking into account the joint effect of shadowing and fast fading can be written, using Eq. 11, as:

$$\begin{aligned}\mathbb{P}\big(\gamma<\delta\big) &= \int_0^\infty \left[1-\mathbb{P}\left(10\log_{10}(\frac{x}{\delta}) > 10\log_{10}(Y_f)\right)\right] p_X(x)dx, \\ &= \int_0^\infty Q\left[\frac{10\log_{10}(\frac{x}{\delta})-m_f}{s_f}\right]e^{-x}dx,\end{aligned} \tag{18}$$

where Q is the error function: $Q(u) = \frac{1}{2}erfc(\frac{u}{\sqrt{2}})$. Eq. 18 represents also the outage probability on a single-carrier.

Remark 2: If we consider only the shadowing effect, the single-carrier outage probability can be written as:

$$\begin{aligned}\mathbb{P}\left(\gamma < \delta\right) &= 1 - \mathbb{P}\left(\frac{1}{\delta} > Y_f(m_f, s_f)\right), \\ &= 1 - \mathbb{P}\left(10\log_{10}(\frac{1}{\delta}) > 10\log_{10}(Y_f)\right), \\ &= Q\left[\frac{10\log_{10}(\frac{1}{\delta}) - m_f}{s_f}\right]. \end{aligned} \tag{19}$$

Remark 3: In Eq. 11, we neglect the variations of the Rayleigh fading for interferers and replace the associated exponential random variables (RV) by their first moment. Another method would be to consider the joint distribution of all RV involved in the interference sum. This approach is much more complex in terms of numerical computation since it would involve N infinite integrals. Although the sum of independent exponential RV has a known distribution (Erlang), the presence of shadowing does not allow to have a closed-form distribution. Another alternative would be to use a gaussian approximation for the entire interference term, but results are much less accurate because RV are positive. In Section 4, we compare the proposed approach with Monte Carlo simulations and show that the approximation is accurate.

We can now come back to the computation of the MIC distribution.

3.3. MIC Distribution

Using the Gaussian approximation, we need to compute the mean μ_{MIC} and the standard deviation σ_{MIC} of the RV MIC (this approach is also used in [24]). These parameters are obtained from order 1 and 2 moments of C_n.

Using Eq. 18, we can write:

$$\begin{aligned} E[C_n] &= \int_0^\infty \mathbb{P}\big(C_n > t)dt, \\ &= \int_0^\infty \big(1 - \mathbb{P}\big(\gamma_n < 2^t - 1)\big)\, dt, \\ &= \int_0^\infty \int_0^\infty (1 - Q_f(x,t))\, e^{-x} dx dt, \end{aligned} \tag{20}$$

with

$$Q_f(x,t) = Q\left[\frac{10\log_{10}(\frac{x}{2^t-1}) - m_f}{s_f}\right]. \tag{21}$$

In the same way:

$$\begin{aligned} E[C_n^2] &= \int_0^\infty 2t\mathbb{P}\big(C_n > t)dt, \\ &= \int_0^\infty \int_0^\infty 2t\,(1 - Q_f(x,t))\, e^{-x} dx dt. \end{aligned} \tag{22}$$

Note that we used here the classical formula for positive RV X and $p \in \mathbb{N}^*$:

$$E[X^p] = \int_0^\infty p t^{p-1} \mathbb{P}\big(X > t)dt.$$

We have indeed from $X = \int_0^\infty \mathbb{1}_{\{t<X\}} dt$:

$$E[X] = E[\int_0^\infty \mathbb{1}_{\{t<X\}} dt] = \int_0^\infty E(\mathbb{1}_{\{t<X\}})dt = \int_0^\infty \mathbb{P}\big(X > t)dt.$$

We obtain the result for $p > 1$ by considering the variable transformation $t = s^p$.

Mean and standard deviation of the MIC are thus given by:

$$\mu_{MIC} = E[C_n], \tag{23}$$

$$\sigma^2_{MIC} = \frac{1}{N_{sc}}(E[C_n^2] - E[C_n]^2). \tag{24}$$

Note that we assumed here that RV C_n are independent. This is a reasonable assumption if we assume that sub-carriers of a sub-channel are uniformly chosen over the system bandwidth, as it is done in diversity modes (PUSC and FUSC in IEEE 802.16 [23]).

Recall that μ_{MIC} and σ_{MIC} depend on the MS distance to its serving BS, r, as m_f and s_f (Eq. 12 and 13).

3.4. Outage Probability

From the MIC distribution, we can now easily deduce the multi-carrier outage probability for a mobile at distance r:

$$\begin{aligned} \mathbb{P}\big(SIR_{eff} < \delta\big) &= \mathbb{P}\big(MIC < \log_2(1+\delta)\big), \\ &= 1 - Q\left[\frac{\log_2(1+\delta) - \mu_{MIC}}{\sigma_{MIC}}\right]. \end{aligned} \tag{25}$$

If the effective SIR and the threshold are expressed in dB, we have the following expression:

$$\begin{aligned} \mathbb{P}\big(SIR_{eff,dB} < \delta_{dB}\big) &= \mathbb{P}\big(SIR_{eff} < 10^{\delta_{dB}/10}\big), \\ &= 1 - Q\left[\frac{\log_2(1+10^{\delta_{dB}/10}) - \mu_{MIC}}{\sigma_{MIC}}\right]. \end{aligned} \tag{26}$$

The location r of mobile u is taken into account in the mean (Eq. 23) and standard deviation (Eq. 24) of the MIC, in the expression of Q_f (Eq. 21), and finally through m_f (Eq. 12) and s_f (Eq. 13). As m_f, s_f, H and G all depend on parameter y_f (Eq. 16), we propose in the next section to use the fluid model in order to compute y_f as a function of r.

3.5. Analytical Fluid Model

In this section, we recall results obtained in [5] for the fluid model. In B, we present the main computation steps and we adapt the notations to the system model presented in this paper. According to the fluid model and assuming that the network is large, y_f can be approximated by:

$$y_f(r,\eta) = \frac{2\pi\rho_{BS}r^{\eta}}{\eta-2}(2R_c - r)^{2-\eta}, \tag{27}$$

where R_c is the half distance between two BS and ρ_{BS} is the BS density.

This closed-form formula allows us to fastly compute functions G and H, parameters m_f and s_f, MIC mean and standard deviation μ_{MIC} and σ_{MIC}, and thus the outage probability for multi-carrier systems.

4. Validation

In this section, we compare the figures obtained with analytical expressions to those obtained by Monte Carlo simulations in a hexagonal network. We also validate our approximations and show the limitation of our formulas.

4.1. Monte Carlo Simulator

The simulator assumes a homogeneous hexagonal network made of 15 rings around a central cell. Fig. 1 shows an example of such a network with the main parameters involved in the study: R, the cell range (1 km), R_c, the half-distance between BS, and R_{nw}, the network size. A reuse 1 network is assumed: all cells use the whole system bandwidth.

For the single-carrier case, the simulation consists of computing at each snapshot the SIR according to Eq. 5 for a uniformly drawn point u of the

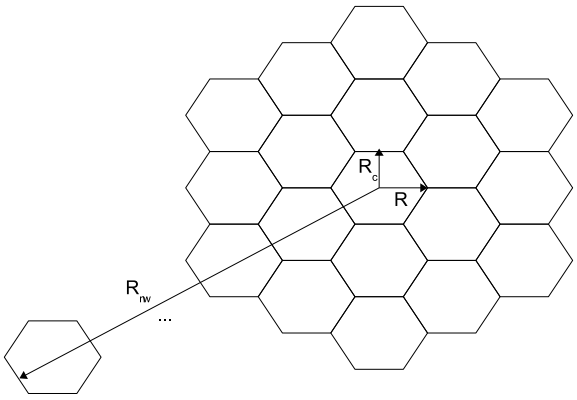

Figure 1: Hexagonal network and main parameters of the study.

central cell. Eq. 5 takes into account path-loss, shadowing and fast fading for the useful signal and for interfering signals. We explicitly compute the distances between user u and all interfering BS.

This computation can be done independently of the number of MS in the cell and of the BS output power (because thermal noise is supposed to be negligible both in simulations and analytical study, and because all BS use the same output power). At each snapshot, shadowing and fast fading RV are independently drawn between the MS and the serving BS and between MS and interfering BS.

For the multi-carrier case, the previous computation is repeated N_{sc} times in order to obtain the γ_n figures. Then, effective SIR is computed using Eq. 8.

SIR (single-carrier) or effective SIR (multi-carrier) samples at a given distance from the central BS are recorded in order to compute the outage probability at a given distance r.

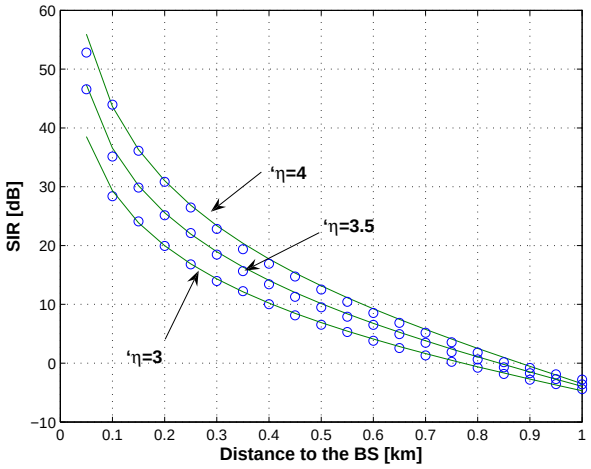

Figure 2: SIR vs. distance to the BS; comparison of the fluid model with simulations on a hexagonal network with $\eta = 3$, 3.5 and 4.

4.2. Validation of the Fluid Model

In this section, we validate the fluid model with Monte Carlo simulations. While reference [7] was focusing on the other-cell interference factor, we focus here on the SIR. To calculate γ, we use the fluid model network approach.

Fig. 2 compares the SIR values given by the fluid model (solid lines), using Eq. 51 to the values of SIR obtained by Monte Carlo simulations (circles) in the hexagonal network. Since η generally ranges from 3 to 4, we present curves for $\eta = 3$, $\eta = 3.5$ and $\eta = 4$. We observe that the two methods provide very close values. The fluid model approach is thus a solid basis for outage probability analysis.

4.3. Single-Carrier Outage Probability

In this section, we validate our outage probability formula (Eq. 18) and compare it to the simulation results obtained in a hexagonal network.

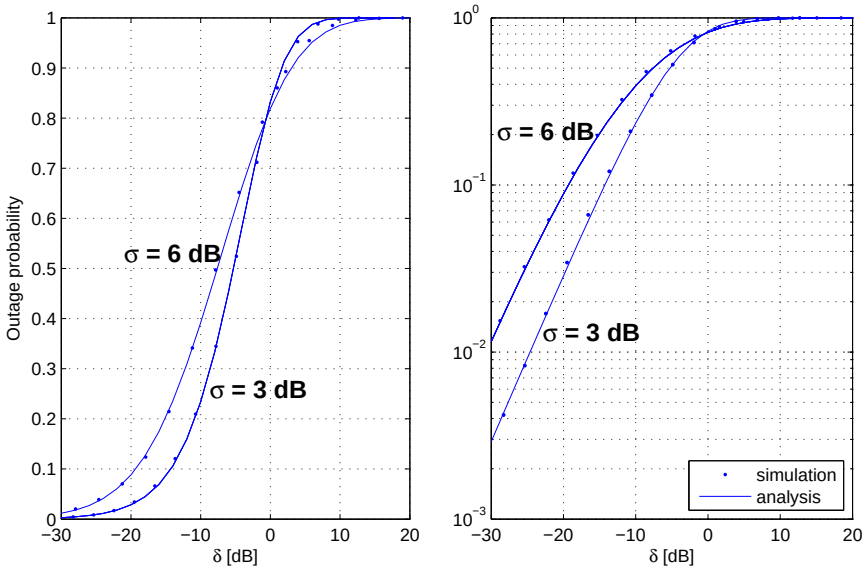

Figure 3: Outage probability for a mobile located at cell edge ($r = R_c$); comparison between analysis (solid curves) and simulations (dotted curves) on a hexagonal network ($\eta = 3$); zoom on the right.

Fig. 3 gives an example of the kind of results we are able to obtain instantaneously. These curves represent the outage probability for a mobile located at the cell edge ($r = R_c$) for path-loss exponent $\eta = 3$, and for two values of σ (3 dB and 6 dB). As an example of interpretation on Fig. 3, for a SIR threshold of $\delta = -15$ dB and a standard deviation of the shadowing of $\sigma = 3$ dB, outage probability is 8 % for a mobile located at the cell edge. We observe that the analytical study provides very good results compared to Monte Carlo simulations, even for low outage probabilities.

Fig. 4 shows the impact of fast fading on the outage probability. The curve with dots takes into account only the shadowing effect (Eq 19), while the curve with crosses considers both shadowing and fast fading impacts

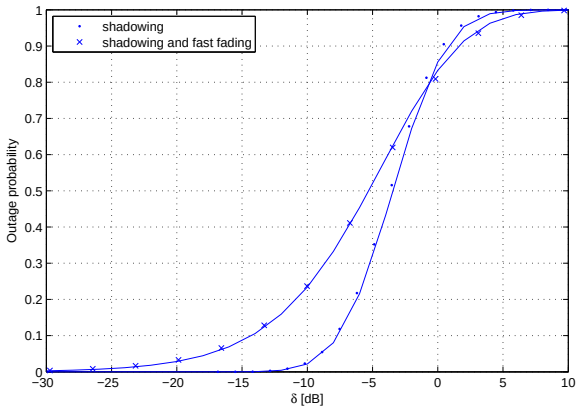

Figure 4: Impact of fast fading on the outage probability for a mobile located at cell edge ($r = R_c$, $\eta = 3$, $\sigma = 3$ dB), dotted curves are obtained with simulations solid ones with analysis.

(Eq 18). Solid curves are obtained with analytical formulas. At 10 % of outage, there is a 7 dB difference between two curves. This illustrates the importance of considering fast fading in dimensioning processes.

4.4. Multi-Carrier Outage Probability

We now consider the multi-carrier case. Fig. 5 and 6 show the outage probability at cell edge ($r = R_c$) and inside the cell ($r = R_c/2$), resp. for $\sigma =$ 3 dB and 6 dB. In all cases, the difference between analysis and simulation results in a hexagonal network is less than 0.5 dB. This accuracy confirms that the gaussian approximation considered in Section 3.3 is efficient for dimensioning purposes.

Fig. 7 shows the SIR threshold obtained at 2% outage, inside the cell ($r = R_c/2$), with single and multi-carrier systems, as a function of the shadowing standard deviation. Analysis and simulation are compared: in all cases and

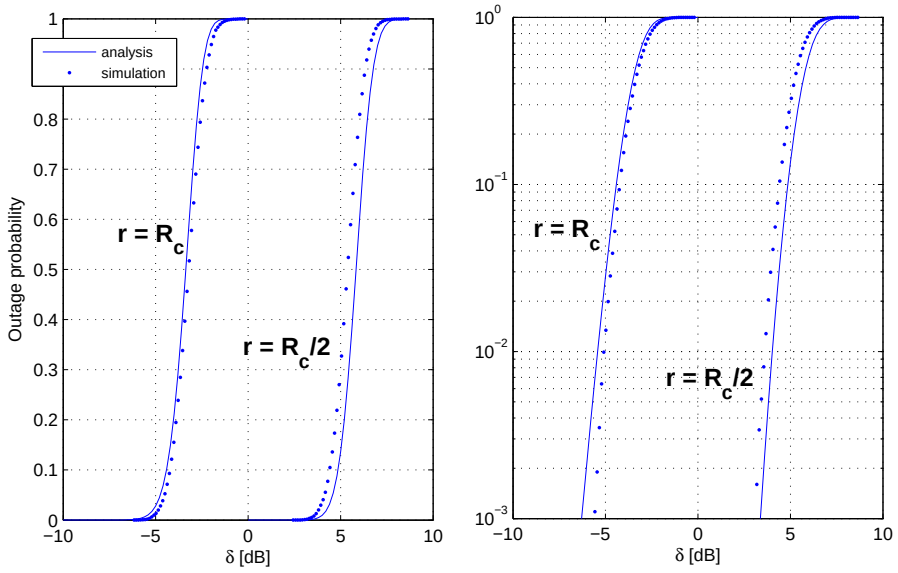

Figure 5: Outage probability at cell edge ($r = R_c$) and inside the cell ($r = R_c/2$); comparison between analysis (solid curves) and simulations (dotted curves) on a hexagonal network ($N_{sc} = 48$, $\eta = 3$, $\sigma = 3$ dB).

in the considered interval, difference is less than 1 dB between analysis and simulation. We clearly see the advantage of using multi-carrier instead of single-carrier. For example, for $\sigma = 4$ dB, there is a 15 dB difference at 2% outage for 48 sub-carriers. The gain is increasing with standard deviation and with the number of sub-carriers per sub-channel.

5. Application to the Dimensioning of a Streaming Service

Our analytical framework allows us to analyze instantaneously the impact of the various parameters involved in the dimensioning of cellular OFDMA networks. This includes environment parameters (shadowing, fast fading, path-loss exponent), network and system parameters (cell range and BS den-

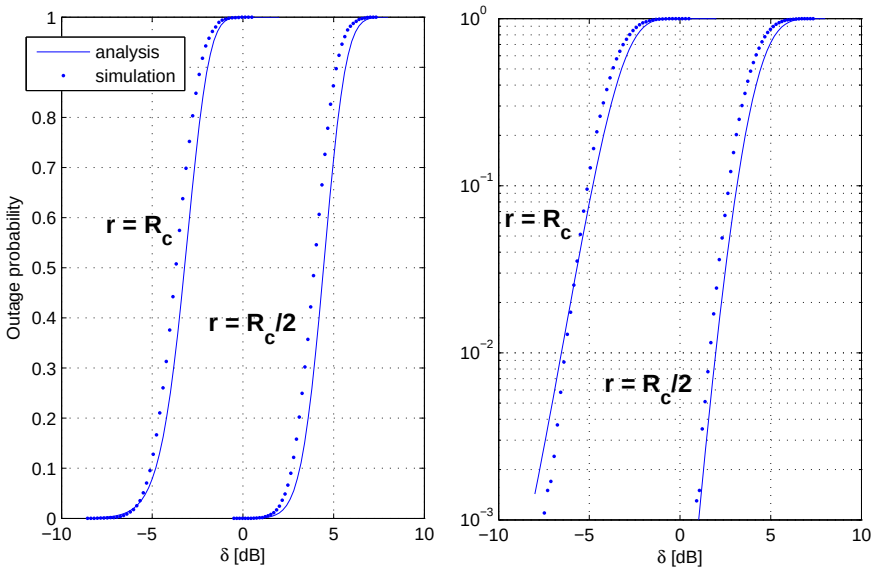

Figure 6: Outage probability at cell edge ($r = R_c$) and inside the cell ($r = R_c/2$); comparison between analysis (solid curves) and simulations (dotted curves) on a hexagonal network ($N_{sc} = 48$, $\eta = 3$, $\sigma = 6$ dB).

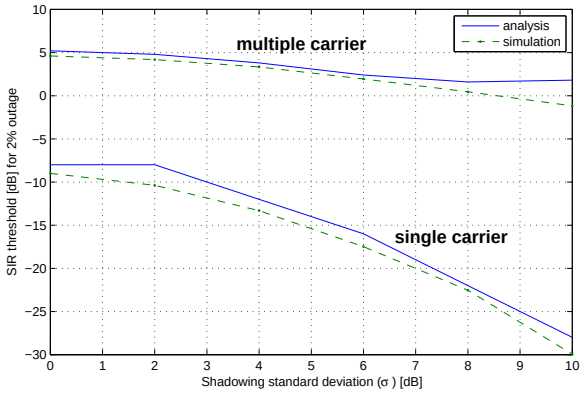

Figure 7: SIR threshold δ in the cell ($r = R_c/2$) for 2% outage probability as a function of the shadowing standard deviation; comparison between analysis (solid curves) and simulations (dotted curves) on a hexagonal network ($N_{sc} = 48$, $\eta = 3$).

sity, number sub-carriers per sub-channel, MS location), and QoS parameters (capacity, effective SIR and related outage probabilities). In this section, we illustrate the latter point by considering an operator willing to offer a service with QoS defined by a target throughput of $\tilde{D}$ kbps and an associated outage probability P_{out} (e.g. a streaming service).

5.1. Outage Capacity

A first simple application of our study is the determination of the outage capacity. Sub-channel capacity is here defined as

$$C_{ch} = N_{sc} W_{sc} \log_2(1 + SIR_{eff}), \tag{28}$$

where W_{sc} is the sub-carrier bandwidth. Fig. 8 shows the outage capacity for different numbers of sub-carriers and $W_{sc} = 11$ kHz, which is the sub-carrier bandwidth in IEEE 802.16e OFDMA. For example, 98% of the users reach more than 2 Mbps at 200 m from the BS if $N_{sc} = 48$ sub-carriers are used per sub-channel.

With this kind of curve, the operator is able to know at each distance which capacity can be guaranteed with a target outage probability. This result is particularly needed for streaming services, for which the average capacity is not sufficient in the dimensioning process.

5.2. Sub-carrier Allocation

The question arises of knowing how many sub-carriers should be allocated to each MS or sub-channel in order to reach the targeted QoS. According to

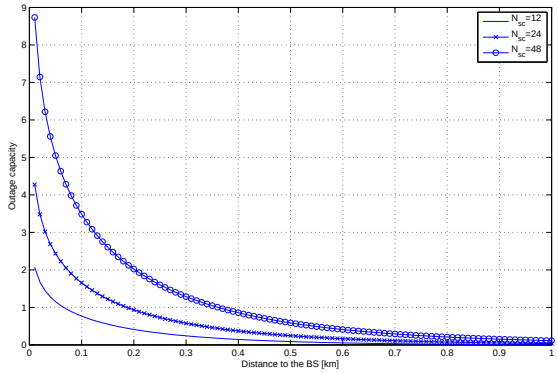

Figure 8: Outage capacity (2%) as a function of the distance to the serving BS (W_{sc} = 11 kHz, $\eta = 3$, $\sigma = 6$ dB).

Eq. 28 and 26:

$$\begin{aligned} P_{out} &= \mathbb{P}\big(C_{ch} \leq \tilde{D}\big), & (29)\\ &= \mathbb{P}\big(SIR_{eff} \leq 2^{\frac{\tilde{D}}{N_{sc}W_{sc}}} - 1\big), & (30)\\ &= 1 - Q\left[\frac{\frac{\tilde{D}}{N_{sc}W_{sc}} - \mu_{MIC}}{\frac{\sigma'_{MIC}}{\sqrt{N_{sc}}}}\right], & (31) \end{aligned}$$

where $\sigma'_{MIC} = \sqrt{N_{sc}}\sigma_{MIC}$. The solution of this equation is given by (see C):

$$\begin{aligned} N_{sc} &= \frac{\tilde{D}}{W_{sc}\mu_{MIC}} \\ &+ \left[\frac{A\sigma'}{\sqrt{2}\mu_{MIC}}\right]^2 \left[1 + \epsilon\left[1 + \frac{4\tilde{D}\mu_{MIC}}{W_{sc}A^2\sigma'^2_{MIC}}\right]^{\frac{1}{2}}\right], & (32) \end{aligned}$$

where $A = Q^{-1}(1 - P_{out})$ and $\epsilon = \pm 1$. $\epsilon = +1$ if $P_{out} < 0.5$; $\epsilon = -1$ if $P_{out} > 0.5$. If $P_{out} = 0.5$, then $N_{sc} = \frac{\tilde{D}}{W_{sc}\mu_{MIC}}$. Recall that μ_{MIC} and σ'_{MIC} are defined for a certain distance r from the base-station.

The first term of the RHS of Eq. 32 is simply the average number of sub-carriers needed to reach throughput $\tilde{D}$ at distance r. The second term is a corrective term that takes into account the requirement in terms of outage probability.

5.3. Capacity/Coverage Trade-off

In this subsection, we illustrate the trade-off between coverage and capacity with regards to the number of sub-carriers per sub-channel.

Each active MS is assigned a unique sub-channel and traffic is here quantified by the density of active MS, computed in a disk of radius r with the following formula:

$$\rho_{MS} = \frac{N_{sc}^T/N_{sc}}{\pi r^2}, \tag{33}$$

where N_{sc}^T is the total number of sub-carriers and N_{sc}^T/N_{sc} can be interpreted as the maximum number of simultaneous MS transfers.

In order to study the effect of a traffic increase on coverage, we compare in Fig. 9 three strategies for the sub-carriers allocation to sub-channels:

Strategy 1 (ECS): Equal and constant sub-channel sizes. We compute the number of needed sub-carriers N_{sc} (Eq. 32) at cell edge ($r = R_c$) and allocate this number of sub-carriers to all MS whatever their location in the cell. The number of active MS is thus constant equal to N_{sc}^T/N_{sc}. This defines a maximum MS density the network (Eq. 33 with $r = R_c$) can bear without coverage holes. When the MS density increases, strategy 1 keeps the sub-channel size constant; the coverage range is thus reduced because the number of active MS is constant; coverage holes appear. The dotted line of Fig. 9 represents the coverage range, r, as a function of ρ_{MS} with N_{sc} constant.

Strategy 2 (EVS): Equal and variable sub-channel sizes. Like for strategy 1, we compute the number of needed sub-carriers N_{sc} at cell edge ($r = R_c$) and allocate this number of sub-carriers to all MS whatever their location in the cell. Contrary to strategy 1 however, when the MS density increases, the sub-channel size is recomputed at the new coverage range. The solid line with circle marks of Fig. 9 is obtained by applying strategy 1 on a disk of radius r, the coverage range.

Strategy 3 (ACS): Adaptive sub-channel sizes. The number of sub-carriers is allocated to MS according to their location, i.e., to their distance to the base-station. The closer is the MS to the BS, the lower is the required number of sub-carriers per sub-channel. The solid line with square marks of Fig. 9 is obtained by computing the *average* number of required sub-carriers over a disk of radius r, the coverage range, and using Eq. 33.

Fig. 9 shows the influence of traffic increase on the coverage range for the three strategies, $\tilde{D} = 256$ kbps, $P_{out} = 2\%$, $R_c = 1$ km and $N_{sc}^T = 1536$. Up to a MS density of $\rho_{MS} = 7.6$ MS/km^2, strategies 1 and 2 ensures a continuous coverage of the service. Thanks to the sub-channel size adaptation, strategy 3 can support a MS density of 12.8 MS/km^2.

As ρ_{MS} increases, coverage range decreases, only MS close to the base-station can still be served. As an example, for $\rho_{MS} = 20$ MS/km^2, coverage ranges are about 0.61 km, 0.78 km and 0.88 km resp. for strategies 1, 2 and 3.

5.4. Network Densification

In the previous section, the inter-BS distance and thus R_c has always been kept constant. A solution to cope with traffic increase consists of densifying

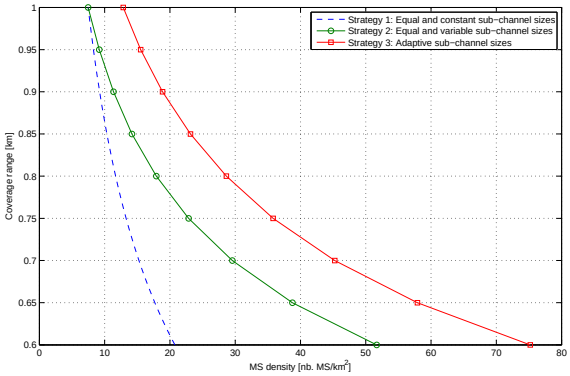

Figure 9: Effect of MS density increase on the cell coverage with a fixed number of sub-carriers per subchannel (solid) or with variable number of sub-carriers (circles) ($\tilde{D}$ = 256 kbps, $P_{out} = 2\%$, $W_{sc} = 11$ kHz, $\sigma = 6$ dB, $R_c = 1$ km).

the network, i.e., increasing the BS density and so decreasing the cell range R_c. In Fig. 10, we plot the strategy 3 curve obtained in the last section (solid curve with squares, fixed BS density). We also plot two curves along with BS density is variable (solid and dotted curves with crosses).

We still assume that the operator has dimensioned his network for a streaming service requiring $\tilde{D} = 256$ kbps guarantee with $P_{out} = 2\%$ and for an initial MS density of 12.85 MS/km^2 (as shown on the figure on the upper left point of the curve). As in the previous section, when MS density increases, e.g. to 23.15 MS/km^2, coverage holes appear, the coverage range is reduced to 850 m (system follows the fixed BS density curve).

To combat this phenomenon and to reach again a full coverage, the operator has two choices: (a) it can keep the same QoS requirement and highly densify the network (new cell range is $R_c = 750$ m; on the figure, the system jumps to the solid line with crosses); or (b) it decides to reduce the QoS re-

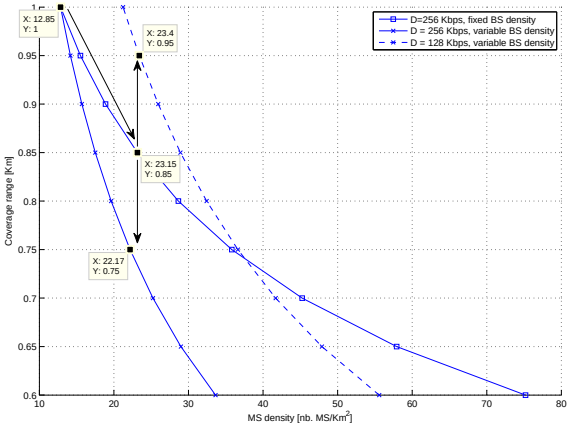

Figure 10: Network densification example ($\tilde{D}$ = 256 kbps and 128 kbps, P_{out} = 2%, $W_{sc} = 11$ kHz, $\sigma = 6$ dB, strategy 3).

quirement to 128 kbps and densify the network (but with a higher cell range of about $R_c = 950$ m, the system jumps to the dotted line with crosses).

These two curves have been obtained by varying R_c in Eq. 50 and using strategy 3 for two different target throughputs and a full coverage ($r = R_c$ in Eq. 32).

Fig. 11 shows the impact of the outage probability and of the path-loss exponent on the cell capacity as a function of the half-distance between BS, R_c. All curves show that decreasing R_c, i.e., densifying, increases the network capacity. Decreasing the QoS constraint from $P_{out} = 2\%$ to $P_{out} = 10\%$ or $P_{out} = 20\%$ allows an increase of the network capacity of resp. 19% and 32% (Fig. 11 left).

As it is well known, network capacity increases with the path-loss exponent because the influence of the interferers is lower. With our analysis, we are able to easily quantify the impact of the environment. For example,

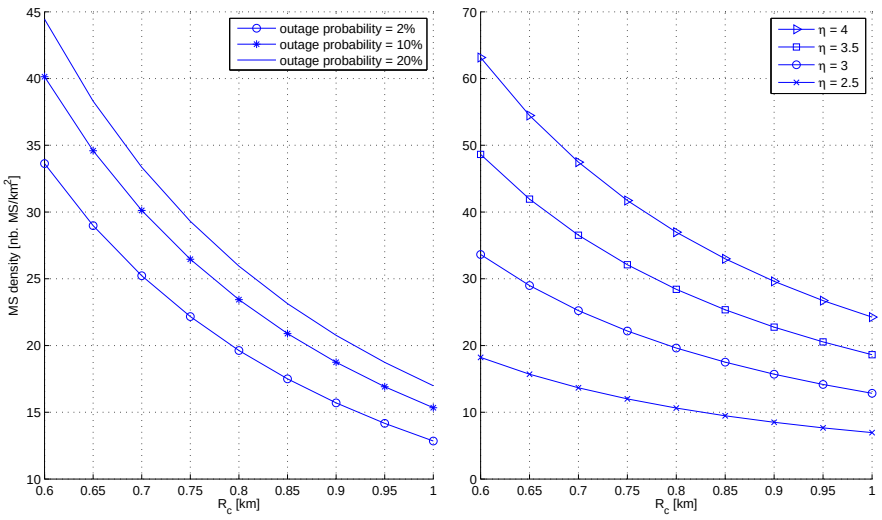

Figure 11: Influence of the outage probability (left) and the path-loss exponent (right) on the cell capacity as a function of the half-distance between BS ($\tilde{D} = 256$ kbps, $W_{sc} =$ 11 kHz, $\sigma = 6$ dB, strategy 3) $\eta = 3$ (left), $P_{out} = 2\%$ (right).

going from $\eta = 3$ to $\eta = 3.5$ leads to a 45% increase for the network capacity (Fig. 11 right).

6. Conclusion

In this paper, we propose and validate by Monte Carlo simulations an analytical model for the performance estimation of cellular OFDMA networks. We address the issue of finding an easy-to-use formula for the outage probability, while considering the joint effect of path-loss, shadowing and fast fading. Firstly considering the notion of MIC, we rely on the Gaussian approximation to express the SIR distribution as a function of the mean and standard deviation of the SIR on a generic sub-carrier. We then analyze the

single-carrier case in order to provide simple formulas of these two moments. At last, the fluid model allows us to obtain expressions that only depend on the distance to the serving BS. Monte Carlo simulations show that our assumptions are valid for a wide range of parameters. The formulas derived in this paper allow to obtain performances results instantaneously. As an example of application, we propose an analysis of the outage capacity, coverage and densification of a network offering a streaming service.

A. Interference Power

The power received from BS j by a MS at distance r_j is a log-normal RV Z_j defined by $\ln(Z_j) \propto N(am_j, a^2\sigma_j^2)$. We can write $m_j = \frac{1}{a}\ln(P_j r_j^{-\eta})$ (to simplify the calculation we consider $K = 1$).

The total power received from interfering BS is expressed as a lognormal RV W (according to the Fenton-Wilkinson approach [1]) defined by $\ln(W) \propto N(am, a^2\sigma_t^2)$ and we can write:

$$am = \ln\left(\sum_{j=1}^{N} e^{(\ln P_j - \eta \ln r_j + \frac{a^2\sigma_j^2}{2})}\right) - \frac{a^2\sigma_t^2}{2}. \tag{34}$$

Assuming that $\forall j\ P_j = P_0$ and $\sigma_j = \sigma$:

$$am = (\ln P_0 + \frac{a^2\sigma^2}{2}) + \ln(\sum_{j=1}^{N} e^{-\eta \ln r_j}) - \frac{a^2\sigma_t^2}{2}. \tag{35}$$

We can now express the mean interference power $\overline{P_{ext}}$ received by a MS as:

$$\ln(\overline{P_{ext}}) = (\ln P_0 + \frac{a^2\sigma^2}{2}) + \ln(\sum_{j=1}^{N} r_j^{-\eta}) - \frac{a^2\sigma_t^2}{2}. \tag{36}$$

The variance $a^2\sigma_t^2$ of the sum of interferences is written as:

$$a^2\sigma_t^2 = \ln\left(\frac{\sum_j e^{(2am_j+a^2\sigma^2)(e^{a^2\sigma^2}-1)}}{(\sum_j exp^{am_j+\frac{a^2\sigma^2}{2}})^2}+1\right). \tag{37}$$

Introducing

$$G(\eta) = \frac{\sum_{j=1}^{N} r_j^{-2\eta}}{\left(\sum_{j=1}^{N} r_j^{-\eta}\right)^2}, \tag{38}$$

the mean value of the total interference received by a mobile is given by

$$\overline{P_{ext}} = P_0 \sum_{j=1}^{N} r_j^{-\eta} e^{\frac{a^2\sigma^2}{2}} \left((e^{a^2\sigma^2}-1)G(\eta)+1\right)^{-1/2}, \tag{39}$$

and

$$a^2\sigma_t^2 = \ln\left((e^{a^2\sigma^2}-1)G(\eta)+1\right) + \ln\left(e^{a^2\sigma^2}\right). \tag{40}$$

We denote P_{int} the power received by a MS from its serving BS. Since the ratio of two lognormal RV's is also a lognormal RV, we can write the following mean:

$$M_f = \frac{\overline{P_{ext}}}{\overline{P_{int}}} \tag{41}$$

and thus, considering that MS is at distance r from its serving BS, we can write:

$$M_f = \frac{\sum_j r_j^{-\eta}}{r^{-\eta}} e^{\frac{a^2\sigma^2}{2}} \left((e^{a^2\sigma^2}-1)G(\eta)+1\right)^{-1/2}. \tag{42}$$

Finally, denoting:

$$H(\sigma) = e^{\frac{a^2\sigma^2}{2}} \left((e^{a^2\sigma^2}-1)G(\eta)+1\right)^{-1/2}, \tag{43}$$

we have

$$M_f = y_f(\eta)H(\sigma). \tag{44}$$

In dB, we can express

$$m_f = \frac{1}{a}\ln(y_f(\eta)H(\sigma)). \tag{45}$$

In a analogue analysis, the standard deviation is given by $a^2 s_f^2 = a^2\sigma_t^2 + a^2\sigma^2$ so we have

$$a^2 s_f^2 = 2(a^2\sigma^2 - ln(H(\sigma))). \tag{46}$$

B. Analytical Fluid Model

In this section, we recall results obtained in [5] and we adapt the notations to the system model presented in this paper. From Eq. 16, we can write:

$$y_f(r,\eta) = \frac{\sum_{j\neq 0} r_j^{-\eta}}{r^{-\eta}} = \frac{\sum_{j\neq 0} P_0 r_j^{-\eta}}{P_0 r^{-\eta}}. \tag{47}$$

The numerator of y_f represents the total power $P_{ext,u}$ received by MS u coming from all the other BS of the system. The denominator of y_f represents the total power $P_{int,u}$ received by MS u coming from its serving BS.

The key modelling step of the fluid model approach developed in [7] for CDMA networks consists of replacing a given fixed finite number of BS by an equivalent continuum of transmitters which are uniformly distributed with density ρ_{BS}.

We focus on a given cell and consider a round shaped network around this centre cell with radius R_{nw}. The half distance between two BS is R_c (see Fig. 12). Let's consider a mobile u at a distance r_u from its serving BS. In our model, each elementary surface $zdzd\theta$ at a distance z from u contains $\rho_{BS} zdzd\theta$ base stations which contribute to $P_{ext,u}$. Their contribution to the external interference is $\rho_{BS} zdzd\theta P_0 K z^{-\eta}$ ($\eta > 2$). We approximate the

integration surface by a ring with centre u, inner radius $2R_c - r_u$, and outer radius $R_{nw} - r_u$ (see Fig. 13):

$$P_{ext,u} = \int_0^{2\pi} \int_{2R_c - r_u}^{R_{nw} - r_u} \rho_{BS} P_0 K z^{-\eta} z dz d\theta,$$

$$= \frac{2\pi \rho_{BS} P_0 K}{\eta - 2} \left[(2R_c - r_u)^{2-\eta} - (R_{nw} - r_u)^{2-\eta} \right]. \quad (48)$$

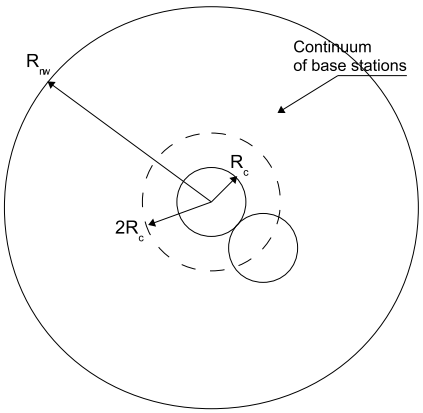

Figure 12: Network and cell of interest in the fluid model; the distance between two BS is $2R_c$ and the network is made of a continuum of base stations.

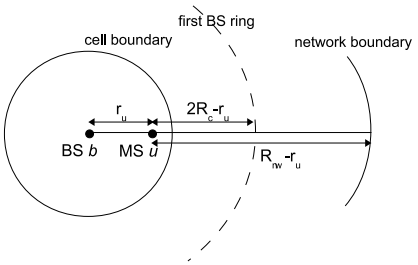

Figure 13: Integration limits for external interference computation.

Moreover, MS u receives internal power from the serving BS, which is at distance r_u: $P_{int,u} = P_0 K r_u^{-\eta}$. So, the parameter $y_f = P_{ext,u}/P_{int,u}$ can be

expressed by (dropping the index u):

$$y_f(r,\eta) = \frac{2\pi\rho_{BS}r^{\eta}}{\eta-2}\left[(2R_c-r)^{2-\eta} - (R_{nw}-r)^{2-\eta}\right]. \tag{49}$$

The closed-form formula of $y_f(r)$ given by the fluid model is validated by comparison with simulations in Section 4.2.

Compared to Eq. 16, we have now an expression of y_f that does not depend any more on the distances to the interferers $\{r_j\}_{j\neq 0}$ but only on the distance r to the BS.

If the network is large, i.e., R_{nw} is big in front of R_c, y_f can be further approximated by:

$$y_f(r,\eta) = \frac{2\pi\rho_{BS}r^{\eta}}{\eta-2}(2R_c-r)^{2-\eta}. \tag{50}$$

We notice that y_f represents the inverse of the SIR without shadowing or fast fading. So we can write from Eq. 50:

$$\gamma = \frac{\eta-2}{2\pi\rho_{BS}r^{\eta}(2R_c-r_u)^{2-\eta}}. \tag{51}$$

This closed-form formula allows us to fastly compute functions G and H, parameters m_f and s_f, MIC mean and standard deviation μ_{MIC} and σ_{MIC}, and thus outage probabilities for single and multi-carrier systems.

C. Computation of N_{sc}

Eq. 29 is equivalent to the following:

$$\frac{\tilde{D}}{\sqrt{N_{sc}}W_{sc}\sigma'_{MIC}} - \frac{\mu_{MIC}\sqrt{N_{sc}}}{\sigma'_{MIC}} = A. \tag{52}$$

Since the function $f(x) = \frac{\tilde{D}}{\sqrt{x}W_{sc}\sigma'_{MIC}} - \frac{\mu_{MIC}\sqrt{x}}{\sigma'_{MIC}}$ is strictly decreasing on $]0;+\infty[$ and takes values in $]-\infty;+\infty[$, there is a unique solution. Then taking the square of both sides:

$$W_{sc}^2\sigma_{MIC}^{'2}N_{sc}^2 - (2W_{sc}\tilde{D}\mu_{MIC} + W_{sc}^2\sigma_{MIC}^{'2}A^2)N_{sc} + \tilde{D}^2 = 0. \qquad (53)$$

This equation has two solutions given by Eq. 32. If $A < 0$, i.e. $P_{out} < 0.5$, then $N_{sc} > \tilde{D}/W_{sc}\mu_{MIC}$ according to Eq. 52, the second term of RHS of Eq. 32 should be positive and $\epsilon = 1$.

References

[1] L. Fenton, The Sum of Lognormal Probability Distributions in Scatter Transmission System, IEEE (IRE) Transactions on Communications, CS-8, 1960.

[2] S. Shwartz and Y.S. Yeh, On the Distributions Functions and Moments of Power Sums with Lognormal Components, Bell Syst, Tech J., Vol. 61, Sept. 1982.

[3] G.L. Stuber, Principles of Mobiles Communications, Norwell , MA. Kluwer, 1996.

[4] Adnan A. Abu-Dayya and Norman C. Beaulieu, Outage Probabilities in the Presence of Correlated Lognormal Interferers, IEEE Trans. on Vehicular Technology, Vol. 43, No. 1, Feb. 1994.

[5] J.-M. Kelif and E. Altman, Downlink Fluid Model of CDMA Networks, Proc. of IEEE VTC Spring, May 2005.

[6] J.-M. Kelif, Admission Control on Fluid CDMA Networks, Proc. of IEEE WiOpt, Apr. 2006.

[7] J.-M. Kelif, M. Coupechoux, and P. Godlewski, Spatial Outage Probability for Cellular Networks, Proc. of IEEE Globecom, Nov. 2007.

[8] J.-M. Kelif, M. Coupechoux, and P. Godlewski, A Fluid Model for Performance Analysis in Cellular Networks, EURASIP Journal on Wireless Communications and Networking, Vol. 2010, Article ID 435189, 2010.

[9] C. C. Chan and Hanly, Calculating the Outage Probability in CDMA Network with Spatial Poisson Traffic, IEEE Trans. on Vehicular Technology, Vol. 50, No. 1, Jan. 2001.

[10] S. E. Elayoubi and T. Chahed, Admission Control in the Downlink of WCDMA/UMTS, Lect. notes comput. sci., Springer, 2005.

[11] J. S. Evans and D. Everitt, On the Teletraffic Capacity of CDMA Cellular Networks, IEEE Trans. on Vehicular Technology, Vol. 48, No. 1, Jan. 1999.

[12] M. Pratesi, F. Santucci, and M. Ruggieri, Outage Analysis in Mobile Radio Systems with Generically Correlated Log-Normal Interferers, IEEE Trans. on Communications, Vol. 48, No. 3, Mar. 2000.

[13] J.-P. M. G. Linnartz, Exact Analysis of the Outage Probability in Multiple-User Mobile Radio, IEEE Trans. on Communications, Vol. 40, No. 1, Jan. 1992.

[14] V. V. Veeravalli and A. Sendonaris, The Coverage-Capacity Tradeoff in Cellular CDMA Systems, IEEE Trans. on Vehicular Technology, Vol. 48, No. 5, Sept. 1999.

[15] G. Immovilli and M. L. Merani, Simplified Evaluation of Outage Probability for Cellular Mobile Radio Systems, IEEE Electronic Letters, Vol. 27, No. 15, Jul. 1991.

[16] T. Bonald and A. Proutiere, Wireless Downlink Data Channels: User Performance and Cell Dimensioning, Proc. of ACM MOBICOM, Sept. 2003.

[17] M Zorzi and S. Pupolin, Outage Probability in Multiple Access Packet Radio Networks in the Presence of Fading, IEEE Trans. on Vehicular Technology, Vol. 43, No. 3, Aug. 1994.

[18] J. Papandriopoulos, J. Evans, and S. Dey, Outage-Based Optimal Power Control for Generalized Multiuser Fading Channels, IEEE Trans. on Communications, Vol. 54, No. 4, Apr. 2006.

[19] A. Williamson and J. Parsons, Outage Probability in a Mobile Radio System Subject To Fading and Shadowing, IEEE Electronics Letters, Vol. 21, No. 14, Jul. 1985.

[20] N. Damji and T. Le-Ngoc, Adaptive Downlink Resource Allocation Strategies for Real-Time Data Services in OFDM Cellular Systems, EURASIP Journal on Wireless Communications and Networking, Vol. 2006, Article ID 17526, 2006.

[21] R. Giulianoand and F. Mazzenga, Dimensioning of OFDM/OFDMA based Cellular Networks using Exponential Effective SINR, IEEE Trans. on Vehicular Technology, Vol. 58, No. 8, Oct. 2009.

[22] WiMAX Forum, WiMAX System Evaluation Methodology, version 2.1, Jul. 2008.

[23] IEEE, Standard for Local and Metropolitan Area Networks, Part 16, Amendment 2: Physical and Medium Access Control Layers, 2005.

[24] A. Clark, P. J. Smith, and D. P. Taylor, Instantaneous Capacity of OFDM on Rayleigh-Fading Channels, IEEE Trans. on Information Theory, Vol. 53, No. 1, Jan. 2007.

[25] J. Leinonen, J. Hamalainen, and M. Juntti, Performance Analysis of Downlink OFDMA Resource Allocation with Limited Feedback, IEEE Trans. on Wireless Communications, Vol. 8, No. 6, June 2009.

[26] L.-C. Wang and W.-C. Li, Outage Performance Analysis for Fractional Frequency Reused TDD-OFDMA Systems with Asymmetric Traffics, Proc. of IEEE ISITA, Oct. 2010.

[27] K. Seong, M. Mohseni, and J.M. Cioffi, Optimal Resource Allocation for OFDMA Downlink Systems, Proc. of IEEE ISIT, July 2006.

[28] I.C. Wong and B.L. Evans, Optimal Downlink OFDMA Resource Allocation With Linear Complexity to Maximize Ergodic Rates, IEEE Trans. on Wireless Communications, Vol. 7, No. 3, Mar. 2008.

[29] C. Seol and K. Cheun, A Statistical Inter-Cell Interference Model for Downlink Cellular OFDMA Networks Under Log-Normal Shadowing and Multipath Rayleigh Fading, IEEE Trans. on Communications, Vol. 57, No. 10, Oct. 2009.

[30] F. Wang, A. Ghosh, C. Sankaran, P.J. Fleming, F. Â Hsieh, and S.J. Benes, Mobile WiMAX Systems: Performance and Evolution, IEEE Communication Mag., Vol. 46, No. 10, Oct. 2008.

[31] A. Goldsmith, Wireless Communications, Cambridge University Press, 2005.